

MAGNETIC PROPERTIES OF $\text{YBa}_2\text{Cu}_3\text{O}_{7-\delta}$ MELT TEXTURED SAMPLES PREPARED BY POWDER MELTING PROCESS AND QUENCH AND MELT GROWTH TECHNIQUES

G. PLESCH^{a,*}, A. CIGÁŇ^b, J. MAŇKA^b, A. BUČKULIAKOVÁ^a, F. HANIC^b,
Š. BUCHTA^b, B. ANDRZEJEWSKI^c AND J. STANKOWSKI^c

^aDepartment of Inorganic Chemistry, Faculty of Natural Sciences
Comenius University, 842 15 Bratislava, Slovakia

^bInstitute of Measurement Science, Slovak Academy of Sciences
Dúbravská cesta 9, 842 19 Bratislava, Slovakia

^cInstitute of Molecular Physics, Polish Academy of Sciences
Smoluchowskiego 17, 60-179 Poznań, Poland

(Received January 25, 2000; revised version July 20, 2000)

The microstructure and magnetic properties of the melt textured $\text{YBa}_2\text{Cu}_3\text{O}_{7-\delta}$ samples prepared by the powder melting process, in which $\text{Y}_2\text{Cu}_2\text{O}_5$ and BaCuO_2 were used as precursors, and those prepared by the quench and melt growth method are described and compared. The lattice parameters and T_c values for the samples prepared by the both techniques were similar. The penetration and the spatial distribution of the magnetic flux in the superconducting samples was imaged by means of a field-mapping device using a Hall probe. In the range of low magnetic fields up to 820 A m^{-1} no significant differences in penetration of magnetic flux between the samples prepared by the powder melting process and the quench and melt growth were observed. The mapping could not resolve any grain boundaries, single grains and structural defects. By the ac and virgin volume magnetisation characteristics, which were measured in the zero-field cooled condition by a 2nd order SQUID gradiometer, no weak links were identified. Better magnetic properties of the quench and melt growth samples in high magnetic fields can be explained by the differences in microstructure and/or by the risen content of the finely dispersed 211 and Pt containing phases. The increase factor in magnetisation is about 2.5. Some aspects of the Bean model for textured $\text{YBa}_2\text{Cu}_3\text{O}_{7-\delta}$ samples are discussed.

PACS numbers: 74.80.Bj, 74.25.Ha

*corresponding author, e-mail: plesch@fns.uniba.sk

1. Introduction

Melt texturing of the Y–Ba–Cu–O system has been proved to be the most promising technique for the preparation of superconducting bulk material with an increased current density. The most frequently used texturing techniques are the quench and melt growth (QMG) and the powder melting process (PMP) fabrication methods [1]. They differ in the precursors, which serve as a source of the system $Y_2BaCuO_5 + L(3BaCuO_2 + 2CuO)$, from which the textured $YBa_2Cu_3O_{7-\delta}$ grows. The choice of the precursors strongly influences the mechanism of growth and the microstructure of the obtained products and consequently their electric and magnetic properties [1–3].

Although it has been reported that the reaction of $Y_2Cu_2O_5$ and $BaCuO_2$ at 950°C leads to polycrystalline $YBa_2Cu_3O_{7-\delta}$ [4], according to our knowledge these precursors have been not used for the preparation of textured samples. In this paper the microstructure and magnetic properties of the textured $YBa_2Cu_3O_{7-\delta}$ material prepared by the PMP technique, in which $Y_2Cu_2O_5$ and $BaCuO_2$ powders were used as precursors, are described. The ac magnetisation studies and virgin magnetisation curves were used to characterise the magnetic properties. The penetration of the magnetic field was investigated by a field-mapping device using a Hall probe. For comparison with the PMP sample also the textured $YBa_2Cu_3O_{7-\delta}$ material prepared by the QMG method was studied.

2. Subject and methods

2.1. Subject

The pellets fabricated by the PMP technique were prepared from the finely milled mixture of $Y_2Cu_2O_5$ and $BaCuO_2$ powders (molar ratio 1 : 4), which was uniaxially pressed to pellets with a diameter of 1 cm. The samples were fabricated in oxygen atmosphere. The optimal conditions of the synthesis involved a rapid heating ($20^\circ\text{C}/\text{min}$) to 1060°C and a melting period (90 min) at this temperature. Then the temperature fell down to 1000°C within 30 min and the sample was slowly cooled with a temperature gradient of $1^\circ\text{C}/\text{h}$ to 930°C . The probe was then cooled to 550°C and oxygenated for 24 h. The textured $YBa_2Cu_3O_{7-\delta}$ material prepared by the QMG technique was synthesised similarly as described in [5, 6]. In the first step the $YBa_2Cu_3O_{7-\delta}$ precursor was prepared by a standard sintering method, it was then molten in a platinum crucible at 1400°C for 20 min and quenched on a copper plate. In the second step the obtained material was powdered, compacted to pellets with a diameter of 10 mm, which were reannealed in oxygen at 1160°C for 60 min, cooled down to 1000°C within 30 min and subsequently from 1000°C to 930°C with a rate of 1°C h^{-1} . The final oxygenation took place at 550°C for 24 h.

2.2. Methods

The experimental equipment for the powder X-ray diffraction measurements, T_c determination by the four-point method, optical and scanning electron microscopy, and wave dispersion spectroscopy (WDS) microanalysis have been published elsewhere [5, 6].

A home-made field-mapping device was used to study the penetration of the magnetic flux to the PMP and QMG samples. The flux distribution was imaged by means of the cryogenic axial Hall probe. The active probe area was 0.04 mm^2 , whereas its accuracy was equal to 0.8 A m^{-1} . The Hall probe was driven by PC computer controlled on X - Y positioning stage. The X - Y position accuracy was $0.1 \times 0.1 \text{ mm}^2$. The distance between the probe and samples' surface was adjusted manually. To stabilise the temperature of the sample it was mounted on the bulk copper platform. Both the sample and the Hall probe were immersed directly into liquid nitrogen. The field generated in the Helmholtz coils placed outside the liquid nitrogen container was parallel to the sample axis. The experiments were performed at 80, 130, 300, 480 and 820 A m^{-1} . All flux images were performed after zero-field cooling followed by the applying of the magnetic field. The laboratory residual field being equal to approximately 40 A m^{-1} has not been compensated.

The ac and virgin volume magnetisation characteristics were measured in the zero-field cooled condition by a 2nd order SQUID gradiometer with the sample placed outside the helium cryostat [7]. All magnetisation characteristics of the samples were measured at 77 K in the range of magnetic fields (10^{-1} – 2×10^5) A m^{-1} . For ac magnetisation measurements the frequency of 0.1 Hz has been used and applied magnetic field H_a was being gradually increased for five amplitudes for a given range. For both ac and virgin magnetisation the applied magnetic field was parallel to the axis of the samples. From the linear behaviour of the virgin dc magnetisation curves in the full Meissner shielding region for the whole sample, the first penetration magnetic field H_{pl}^{wl} and magnetic susceptibility χ were determined. The first penetration field H_{pl}^{wl} was determined as the field of the first deviation from the linear field dependence of the virgin magnetisation curve measured in the given range of magnetisation field (where experimentally obtained value of magnetic susceptibility χ corresponds to the perfectly diamagnetic one). This parameter characterises the onset of flux penetration through the sample volume. For ac magnetisation characteristics the demagnetising factor was determined from the sample dimension using the ellipsoid approximation [8].

3. Results and discussion

In the literature the use of precursor mixtures $Y_2O_3/BaCuO_2/CuO$ or $Y_2BaCuO_5/BaCuO_2/CuO$ has been mostly reported for preparation of textured $YBa_2Cu_3O_{7-\delta}$ material by the PMP technique [1, 2]. However, according to [9] the system $Y_2Cu_2O_5/BaCuO_2$ leads in the temperature range of 1025 – 1075°C to a coexistence region of $Y_2BaCuO_5 + CuO + L$, which should be suitable for growing the textured $YBa_2Cu_3O_{7-\delta}$ material. By slow cooling the finely milled mixture of $Y_2Cu_2O_5$ and $BaCuO_2$ powders (molar ratio 1 : 4) through the peritectic temperature we obtained pellets with distinctly developed grains of $YBa_2Cu_3O_{7-\delta}$ in a highly textured microstructure. The samples prepared by the QMG technique were also well textured. According to the results of optical microscopy the pellets consist of several domains of parallel $YBa_2Cu_3O_{7-\delta}$ grains. The domains are separated from each other by cracks and low angle boundaries. Their size increased from 1–2 mm for PMP samples to 2–5 mm for QMG samples. The melting process

led in both cases to a low porosity of 5–10%, which was calculated from the density determined by means of mercury volume displaced from the sample. Pores of the size of 100–200 μm can be observed by optical microscopy. Further also the cracks and microcracks contribute to the porosity. In the investigated samples, beside the superconducting matrix, also other phases were detected by optical polarisation and electron scanning microscopy, which was combined with WDS analysis. Grains of Y_2BaCuO_5 (green phase) with an approximate size of 1–20 μm were finely distributed in the samples. This phase finely dispersed in $\text{YBa}_2\text{Cu}_3\text{O}_{7-\delta}$ plays an important role as pinning centres [1]. Further larger grains of CuO and a mixed Ba/Cu oxide with an irregular shape were found. These phases were formed in the process of the solidification of Y deficient liquid. In contrary to the PMP samples, in the pellets prepared by the QMG technique also Pt-rich phases have been observed. These phases were formed in an interaction with the Pt crucible in the melting period. According to [1] this phase significantly improves the superconducting properties of the textured samples. From the X-ray diffraction measurement the lattice parameters $a = 382.1(12)$ pm, $b = 388.5(12)$ pm, $c = 1167.63(3)$ pm of the orthorhombic unit cell of the PMP sample were determined. They correspond to the fully oxygenated $\text{YBa}_2\text{Cu}_3\text{O}_{7-\delta}$. In accordance with this fact the critical temperature of $T_c = 91$ K was determined by the transport four-point method. The lattice parameters and T_c values for the samples prepared by the PMP and QMG techniques were comparable. According to the X-ray diffraction measurements and the optical microscopy in the material prepared by PMP only small amounts of Y_2BaCuO_5 were present. It was significantly smaller than the amount of Y_2BaCuO_5 in the samples synthesised by the QMG technique, where typically 15–20 mass % of “green phase” has been found [6].

The 3D flux images for PMP and QMG samples for the investigated magnetic fields indicate a homogeneous structure of the samples. Neither inhomogeneities nor grain boundaries are visible. The intergrain critical fields and currents are high enough to prevent flux penetration to the samples. Figure 1 shows some representative flux profiles for PMP and QMG samples determined along the cross line through the sample. The solid lines represent the best fits according to the equation for Meissner ellipsoid [10, 11]. The parameters of the fits are constant for all fields and correspond well to the geometrical dimensions of the samples. The similar dimensions of the samples and Meissner ellipsoids prove the negligible magnetic flux penetration in the range of low magnetic fields up to 820 A m^{-1} .

Figure 2 presents the relation between the applied field H_0 and the minimal field measured over the centre of the sample H_z . The relation between the two fields is linear and can be fitted using the following equation [12]:

$$H_z \approx (4h_p/\pi R)H_0.$$

The value of H_z/H_0 ratio is equal to 0.45 for the PMP sample and close to the value 0.41 calculated from the radius of the sample R and the distance between the Hall probe and the sample surface h_p . For the QMG sample the H_z/H_0 ratio is equal to 0.2 from the fitting whereas the calculated one is equal to 0.15. The linear relation between H_z and H_0 once again points to the absence of the flux penetration in the low fields. The nonlinearity of this relation is usually caused by the flux penetration towards the sample [12].

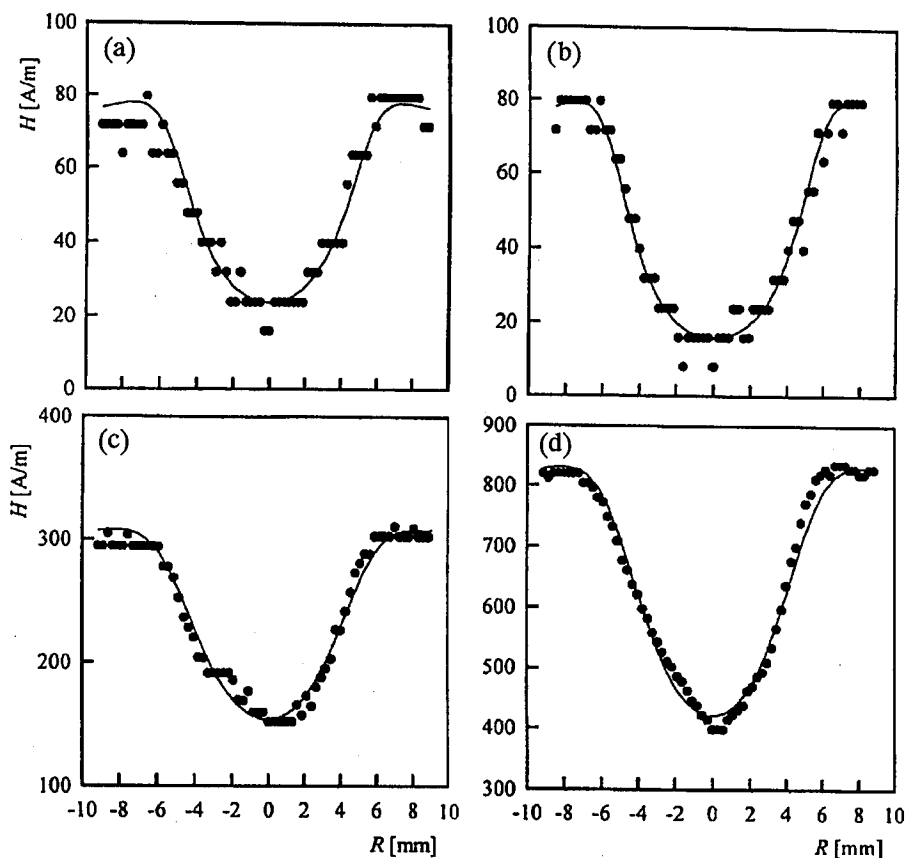


Fig. 1. The flux profiles determined along the cross line through the samples with a diameter R ; (a) PMP sample, $H_0 = 80 \text{ A m}^{-1}$; (b) QMG sample, $H_0 = 80 \text{ A m}^{-1}$; (c) PMP sample, $H_0 = 480 \text{ A m}^{-1}$; (d) PMP sample, $H_0 = 820 \text{ A m}^{-1}$. The solid lines are the best fits according to the equation for the Meissner ellipsoid.

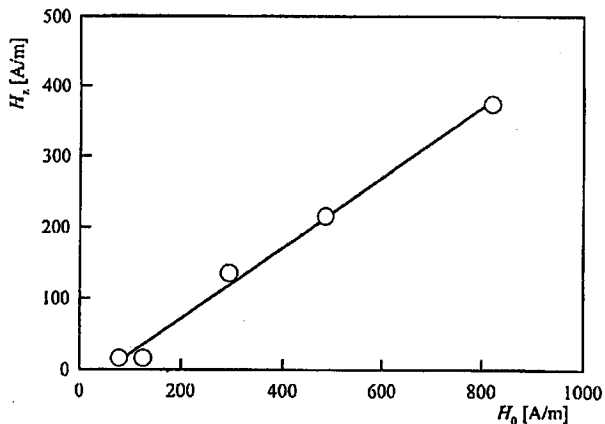


Fig. 2. The field over the centre of the sample H_z versus the applied magnetic field H_0 for PMP sample.

The magnetic flux imaging shows no differences in the magnetic properties between PMP and QMG samples in a low magnetic field range and indicates that both samples screen perfectly the magnetic field up to 820 A m^{-1} . In contrast to the above results it has been reported previously [13] that irregularities in the expelled magnetic field of similar magnitude as used in our case, evidenced structural inhomogeneities in textured samples prepared by the QMG method. This difference can be explained by the fact that the size of the inhomogeneities in our samples is lower as the resolution of the mapping device. Also in [14] the inhomogeneities of the shielded fields above the textured samples have been highly pronounced, however, at external magnetic fields, which were two orders higher than in this work.

Figure 3 shows the ac magnetisation M vs. the applied field H_0 (corrected by the demagnetisation factor) of the sample fabricated by the PMP technique for five magnetisation field amplitudes. The shape of the magnetisation curve documents that the sample is well textured and no weak links can be identified. However, the value of 2.7 kA m^{-1} of the first penetration field H_{pl}^{wl} is relatively small.

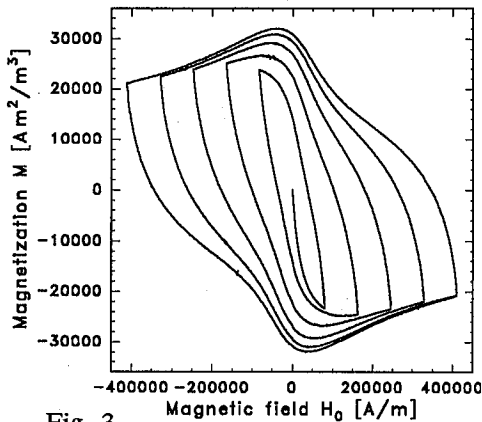


Fig. 3

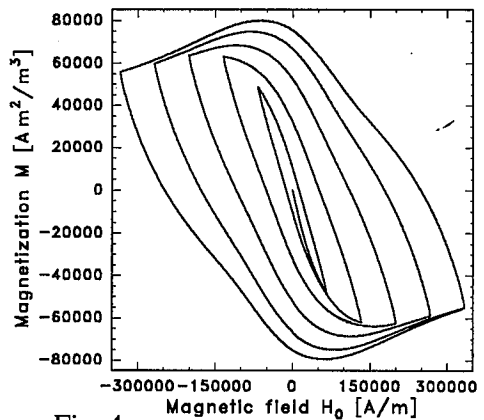


Fig. 4

Fig. 3. The ac magnetisation M vs. the applied field H_0 for the PMP sample.

Fig. 4. The ac magnetisation M vs. the applied field H_0 for the QMG sample.

The ac magnetisation M vs. the applied field H_0 is shown in Fig. 4 for the sample fabricated by the QMG technique for five amplitudes of H_0 . The shape of the magnetisation curve is very similar to that for the PMP sample. The sample has a good texture without weak links. The value of the first penetration field H_{pl}^{wl} is about 10.8 kA m^{-1} . A higher value of H_{pl}^{wl} for the QMG sample indicates its better intergrain or grain properties. The last ones can be connected with the fact that the PMP process led to the pellets with more cracks and microcracks. Magnetisation and magnetisation hysteresis are higher by factor of 2.5 than for the PMP sample. If we would assume that the characteristic dimensions of the shielding current loops are equal to the domain size, according to the Bean critical state model, the critical current densities for the PMP and QMG samples would be comparable.

The correct use of the Bean model for determination of the critical current density from the magnetisation data requires knowledge of the characteristic diameter of the induced current loops in the state of full magnetic flux penetration through the sample. Discussion about the limitations of this model has been reported in [15, 16]. Murakami et al. [15] found that the magnetisation behaviour of their $\text{YBa}_2\text{Cu}_3\text{O}_7$ samples prepared by the QMG method could be described by the Bean critical state model. The supercurrents circulated in the whole sample and weak links were absent. However, on the other hand for $\text{YBa}_2\text{Cu}_3\text{O}_7$ crystals conflicting results were reported. Some data showed a steady increase in magnetisation with the size of crystals or powder particles, while some results showed that the magnetisation was size independent [17, 18]. Yeshurun et al. [17] observed that the remanent magnetisation at low temperatures increased linearly with the crystal size (R) up to a few hundreds of micrometers and sublinearly with larger sizes of R . Others, for example Sulpice et al. [18], found that the magnetisation of $\text{YBa}_2\text{Cu}_3\text{O}_7$ crystals increased sublinearly with R (with saturation at high values) already at low temperatures. Some magnetisation techniques were suggested for testing the Bean critical state model [16, 19]. Angadi et al. [19] based upon the analysis of the initial slopes of the reverse leg of the experimental magnetisation loops.

For our QMG and PMP pellets we estimated the characteristic current length scales as 5.8×10^{-3} m and 5.3×10^{-3} m by a similar way as in [19]. These results are rather close to the values of the samples' radii in the first approximation. This fact indicates that the increased magnetisation and width of the $M(H)$ loop reflect rather better pinning properties of the QMG sample comparing with the one prepared in a PMP process.

4. Conclusion

$\text{Y}_2\text{Cu}_2\text{O}_5$ and BaCuO_2 powders can be effectively used as precursors for powder melt powder synthesis of melt textured $\text{YBa}_2\text{Cu}_3\text{O}_{7-\delta}$ samples. Their lattice parameters, T_c values, microstructure and magnetic properties are comparable to the probes prepared by the standard QMG technique. The magnetisation curves and the magnetic flux imaging performed in low magnetic fields give no evidence for weak links. The observed differences in microstructure and/or in the additional 211 and Pt-containing phase composition is probably the reason for better magnetic properties of the QMG samples. The factor of increase in magnetisation is about 2.5.

Acknowledgment

This work was supported by the Slovak Grant Agency for Science (VEGA Projects No. 1/4087/97 and 2/5086/98) and by the Committee for Scientific Research (Poland) under grant No. 7 T08D 017 15.

References

- [1] M. Murakami, *Prog. Mater. Sci.* **38**, 311 (1994).
- [2] K. Salama, D.F. Lee, *Supercond. Sci. Technol.* **7**, 177 (1994).
- [3] I. Monot, J. Wang, M.P. Delamare, J. Provost, G. Desgardin, *Physica C* **267**, 173 (1996).
- [4] F. Zhaungo, Ji Chunlin, *J. Less-Common Met.* **152**, L5 (1989).
- [5] G. Plesch, F. Hanic, Š. Buchta, A. Rosová, B. Czyżak, B. Andrzejewski, J. Stan-kowski, *Supercond. Sci. Technol.* **9**, 1048 (1996).
- [6] F. Hanic, G. Plesch, Š. Buchta, J. Dobrovodský, L. Danielik, *J. Solid. State Chem.* **116**, 136 (1995).
- [7] V. Zrubec, A. Cigáň, J. Maňka, *Physica C* **223**, 90 (1994).
- [8] J.A. Osborn, *Phys. Rev.* **67**, 351 (1945).
- [9] M. Nevřiva, E. Pollert, J. Šesták, L. Matějková, A. Tríska, *Physica C* **153-155**, 377 (1988).
- [10] S. Reich, V.M. Nabutovsky, *J. Appl. Phys.* **68**, 668 (1990).
- [11] D.A. Brawner, N.P. Ong, *J. Appl. Phys.* **73**, 3890 (1993).
- [12] R. Weinstein, I.-G. Chen, J. Liu, D. Parks, *Appl. Phys. Lett.* **56**, 1475 (1990).
- [13] P. Kottman, M. Polák, J. Pitel, Š. Buchta, L. Danielik, F. Hanic, G. Plesch, *Supercond. Sci. Technol.* **7**, 67 (1994).
- [14] X.H. Jiang, D.M. Astill, W. Lo, D.A. Cardwell, T.A. Coombs, A.M. Campbell, J.G. Larsen, *Physica C* **249**, 171 (1995).
- [15] M. Murakami, M. Morita, N. Koayama, *Jpn. J. Appl. Phys.* **28**, 7, L1125 (1989).
- [16] G.K. Han, K. Watanabe, S. Awaji, N. Kobayashi, K. Kimura, *Physica C* **274**, 33 (1997).
- [17] Y. Yeshurun, M.W. McElfresh, A.P. Malozemoff, J. Hagerhorst-Trewhella, J. Mannhart, F. Holtzber, G.V. Chandrashekar, *Phys. Rev. B* **42**, G322 (1990).
- [18] A. Sulpice, P. Lejay, R. Tournier, J. Chaussy, *Europhys. Lett.* **7**, 365 (1988).
- [19] M.A. Angadi, A.D. Caplin, L.R. Laverty, Z.X. Shen, *Physica C* **177**, 479 (1991).